

Lateral and Feedback Schemes for the Inhibition of False-positive Responses in Edge Orientation Channels

Youngbin Park and Il Hong Suh, Senior Member, IEEE

Abstract—Object recognition is one of the most important applications of robotics. For object recognition, edge orientation is widely used as a primitive visual feature. However, a classical filter-based approach passes not only edges inside target orientation band but also edges outside. This can thus cause problem in the estimation of the true orientation of edge. This study proposes a filtering scheme to reduce the false-positive responses, i.e. edges outside target orientation band, and investigate a solution inspired by biological vision. Motivated by several psychophysical and neuro-physiological findings, we present a computational framework based on the basic mechanisms of cortical processing, i.e. feed-forward, lateral and feedback stages. In the feed-forward stage, our model uses a classical filter-based method to allow as many true orientation edges to pass through as possible. False responses in orientation channels are then inhibited by lateral interaction. The remaining undesired responses are suppressed through the feedback stage. We evaluated the performance of our model against classical filter-based methods such as Gabor and Neumann filtering using several artificial and natural images. The results validated the effectiveness of our approach.

I. INTRODUCTION

Object recognition is one of the most important applications of robotics as it is fundamental for other robotic applications such as localization/navigation, manipulation and human-robot interaction. Edge orientation is widely used as a primitive visual feature for object identification and classification [1], [2], [3], [4]. Precise edge detection is necessary for analyzing edge orientation. Edge detection can be performed before determining orientation [5]. Alternately, edge detection and determination of orientation can be performed simultaneously [6], [7]. Most studies in computer vision have focused on edge detection performance or edge localization [8], [9], [10], [11], and not on the estimation of edge orientation.

Simple gradient-based [12], tensor-based [7] and filter-based [6], [5] schemes are well known approaches for analyzing edge orientation. A simple gradient-based scheme computes the gradient vector at each pixel orientation and the edge orientation is then calculated from the direction of the gradient vector of the pixels. Simple gradient-based scheme is sensitive to noise. While a simple gradient-based scheme describes the local structure at a single position, a tensor-based method also considers the gradients in its neighborhood. The integration of the gradient information in the neighborhood of the pixel helps to determine whether

the pixel is occupied by an edge or a corner and provides increased robustness to noise. The filter-based scheme has recently become the most well known and widely used approach. The filter-based method convolves an input image and a filter tuned for a particular band of orientation.

Gabor filtering (see Section 2.1) and Neumann filtering (see Section 2.2) are filter-based methods that mimic early visual processing in the human brain by computing correlations between the filter and the input signal based on the feed-forward connection. Here, the feed-forward connectivity is implemented by the convolution operation. These two methods can be applied to image containing moderate noise or multiple orientations such as a corner or a crossing. However, we argue that such filtering using classical convolution inevitably passes edges outside of the target orientation band (see 2.3 for details). Consequently, the output orientation channel contains numerous false-positive responses, increasing ambiguity in the estimation of the true orientation.

The main goal of this work is to develop a filtering scheme that reduces such false-positive responses and investigate a solution inspired by biological vision. We selected this approach because humans outperform the best machine vision systems using almost any measure. In fact, several works in the field of low and high level visual applications [5], [3], [4] report that model that have a basis in biological visual systems achieve good performance in various difficult tasks. However, our model does not aim to directly adapt the many physiological and neuro-physiological findings in the visual cortex. Instead, we built our system based on the basic mechanisms of cortical processing.

There is considerable dispute over what the basic mechanisms of cortical processing are. However, multi-stages of processing through feed-forward, lateral and feedback connections is widely acknowledged as the basic processing mechanism [13], [14], [15], [16], [17]. Motivated by the above psychophysical and neuro-physiological observations, we suggest a computational framework involving not only feed-forward connections but also competitive lateral and feedback interactions. The main contribution of this work is to synergistically combine three basic types of connections. This is based on the hypothesis that each type of connection provides different level of information that cannot be conveyed by other types of connections.

We aim to pass only edges approximately within $+22.5$ to -22.5 from the target orientation and to decrease the ratio between the input and output responses of an edge in the form of a Gaussian. The peak of the Gaussian is

Youngbin Park is with the The Department of Electrical and Computer Engineering, Hanyang University, Seoul, Korea pa9301@incorl.hanyang.ac.kr

Il Hong Suh is with the The Division of Computer Sciences and Engineering, Hanyang University, Seoul, Korea ihsuh@hanyang.ac.kr

the center of the target orientation band. Three are eight directions that we need to distinguish in this work, i.e. $0^\circ, 22.5^\circ, 45^\circ, 67.5^\circ, 90^\circ, 112.5^\circ, 135^\circ,$ and 157.5° .

Specifically, our model consists of three layers and three functional processing stages. The first and second layers, which are the input and output layers respectively, interact through the feed-forward connection. This connection is shaped by the convolution operation as used in Gabor and Neumann filtering, processing through this connection is called the feed-forward stage. After this operation, non-negligible false-positive responses inevitably remained in the output orientation channel along with correct responses, as described earlier. However, the aim in this processing stage is to pass as many edges of true orientation as possible even if false-positives are passed through as well. As a result, an additional processing stage is required to inhibit the undesirable responses. Orientation channels in the output layer are connected laterally. After convolution, the maximum response over all orientations is selected at each pixel and some responses below a particular threshold are then inhibited according to the difference in magnitude between the maximum and the target response. This process is lateral inhibition stage. The third layer is the Ω -layer. The output and Ω -layers interact through a feed-forward and feedback connection. This connection encodes some intuition which is relevant to the shape of the responses of the orientation channel in the output layer under the condition that most false-positive responses are inhibited properly. The third processing stage is called inhibitory feedback. After lateral inhibition, each orientation channel is again convolved with 8-oriented filters and the result is fed back to the previous output layer in order to inhibit remaining false-positive responses. It should be noted that in our model such feedback is executed only once.

II. CLASSICAL FILTER-BASED SCHEME FOR ANALYSIS OF EDGE ORIENTATION

Figure. 1 shows responses of convolution with four filters tuned for orientations ($0^\circ, 45^\circ, 90^\circ$ and 135°) in the range of 0 to 255. Here, (a) is the input image, and (b)-(e) are the orientation channels obtained using Neumann filtering ($0^\circ, 45^\circ, 90^\circ$ and 135°). Ideally, each orientation channel should only contain edges that are oriented direction similar to each pair of filters as in (f)-(i). However, we observed that some undesirable pixels are activated in (b)-(e). These can cause ambiguity in object recognition which uses edge orientation as a primitive feature. In this section, the classical filter-based scheme is reviewed using Gabor filtering and Neumann filtering, and problems with the classical filter-based scheme are illustrated.

A. Gabor Filtering

An important insight put forward by Daugman [6] is that simple cells in the visual cortex can be modeled using Gabor functions. The 2D Gabor functions proposed by Daugman are local spatial band-pass filters and they can be tuned to respond to a particular orientation band and scales of

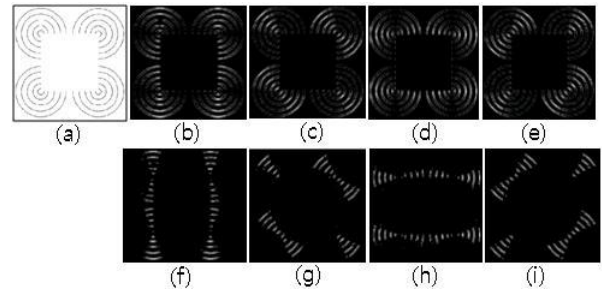


Fig. 1. (a) Original image (b-e) Output images using Neumann filtering (f-i) Output images using proposed filtering method. All response values of output images are in the range 0-255.

edge. Daugman [6] generalized the Gabor function into the following 2D form to model the receptive fields of orientation-selective simple cells:

$$g(x, y) = \exp \left[-\frac{1}{2} \left(\frac{x'^2}{\sigma_x^2} + \frac{y'^2}{\sigma_y^2} \right) \right] \exp(j2\pi u_0 x') \quad (1)$$

$$x' = x \cos \theta + y \sin \theta, \quad y' = -x \sin \theta + y \cos \theta, \quad (2)$$

where u_0 is the wavelength of the sinusoidal factor, θ represents the orientation angle of the Gabor filter, and σ_x and σ_y are the standard deviations of the Gaussian envelope.

From equation (1), we can see that the 2D Gabor function is the product of a Gaussian and a complex plane wave. The filter thus has real and imaginary components representing orthogonal directions. The real part is specified by a cosine modulated by a Gaussian, and the imaginary part is specified by a sine modulated by a Gaussian. The real and imaginary filters are also known as quadrature pairs of even and odd symmetric filters. Even and odd filters selectively detect ridge and step edges respectively, and the combination of both filters allows the adaptive control over phase as well as orientation. A bank of Gabor filters is investigated to separate the input signal into multiple channels where each Gabor filter in the bank is tuned to detect patterns of a specific frequency and orientation. For several vision applications such as texture analysis, stereovision and object recognition, Gabor filtering is often implemented by convolving the input image with a bank of Gabor filters.

B. Neumann Filtering

A plausible biological model for detecting a particular orientation range for edges and contours was proposed by Hansen and Neumann [5]. The model involves two stages. The first stage is the feed-forward stage, which is composed of LGN on-and off cells, and simple and complex cell steps. The second stage is the recurrent long-range interaction stage. In this paper, we focus only on the feed-forward stage, which we call Neumann filtering.

In LGN cells step, a bright pixel surrounded by dark pixels is activated in the on-channel and a dark pixel surrounded by bright pixels is activated in the off-channel. Both channels

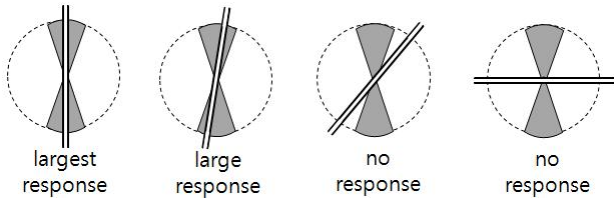


Fig. 2. Responses of the orientation selectivity cell in the visual cortex.

are generated by a difference-of-Gaussians (DOG) operation. Simple cells convolve the on and off channels of LGN through several rotated and elongated Gaussian filters:

$$g(x', y') = \frac{1}{2\pi\lambda\sigma^2} \exp\left[-\frac{(x'/\lambda)^2 - y'^2}{2\sigma^2}\right]. \quad (3)$$

This step generates orientation channels in which pixels within a specific orientation range are activated. Orientation channels are divided into two polarities (darkbright and brightdark) for each orientation. The responses of a complex cell are similar to the responses of a simple cell. The only difference is in the polarity insensitive, since the complex cell generates responses by pooling simple cells of both opposite polarities in each orientation. Thus, responses in each orientation channel at the complex cell step represent a certain edge orientation range and are similar to the responses of an oriented Gabor filter.

A difference between Gabor and Neumann filtering is that while Gabor filtering detects an edge and simultaneously analyzes the edge orientation, Neumann filtering localizes the edge in the LGN cells step and then estimates the orientation in the simple cell step. Another difference is in the shape of the tuning curve. The tuning curve refers to the particular response profile and ideally contains a single peak around the preferred orientation of the filter. The even Gabor filter has positive weights along the main axis of the filter and negative weights around the positive values. This creates sharp tuning curve which is considerably good at preventing edges with false orientation from passing through but can sometimes block true edges. On the other hand, Neumann filtering uses the anisotropic Gaussian, which is composed only of positive weights. Therefore, width of the tuning curve is larger than in the case of Gabor filtering. Thus, edges with false orientation often passed through but true edges are remained as much as possible.

C. Problem Caused by Classical Filter-based Scheme

Figure. 2 shows the responses of an orientation selectivity cell in the visual cortex. The cell is tuned to detect vertical edges. The main axis of the gray region indicates the preferred orientation, and straight lines depict incoming visual data. If the input stimulus is oriented exact or similar to the preferred orientation, the response of the cell is largest or large, respectively. On the other hand, if the input orientation is outside of the preferred orientation band, the response is zero. As mentioned earlier, the classical vision approaches is to convolve the image with the oriented filter to analyze edge

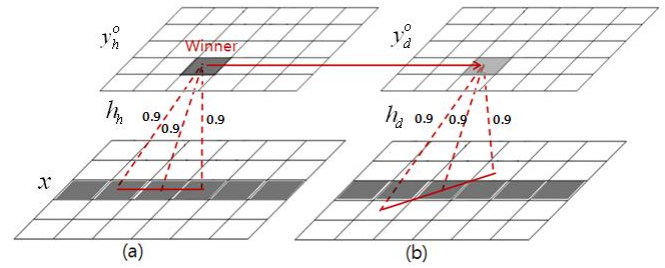


Fig. 3. Convolutions with a simplified version of oriented filters for the sake of brevity. The digits denote weights of the filter. x denotes the input layer, superscript o indicates the output layer, and subscripts h and d indicate the horizontal and diagonal directions, respectively. Dark gray depicts a high activation value while light gray is a low value. (a) Convolution by a horizontal filter. (b) Convolution by a diagonal filter.

orientation. However, there are some differences between the orientation selectivity cell in the visual cortex and the convolution operation in their responses to various input stimuli:

$$y(m, n) = x(m, n) * h(m, n) = \sum_j \sum_i x(i, j) \cdot h(m - i, n - j). \quad (4)$$

In computer vision, Eq. (4) is widely used for convolution. Here, $y(m, n)$ denotes response at pixel (m, n) , x represents input, and h represents filter. According to this equation, if the input values are small y will be small, even though the input edge and the main axis of the filter overlap perfectly. On the other hand, if the value of x is high enough, then y can be larger than in the previous case, even though the input line and the main axis of the filter overlap partially. This is the most important difference between the orientation selectivity cell in the visual cortex and the convolution operation. In other words, the orientation selectivity cell depends only on the orientation of the input stimuli, while convolution depends on both the orientation and intensity. For this reason, filter-based scheme inevitably passes edges outside the target orientation band. The consequences of this problem should be considered during subsequent processing for the estimation of the edge orientation.

For a real image, convolution frequently produces a small response in the first and second cases shown in Fig. 2 and a relatively larger response in the third and fourth cases, referred to as false responses in this paper. Thus, there is no way of determining whether the small response is from a low intensity and input with the preferred orientation or from a high intensity input not having the preferred orientation. we aim to inhibit the response of input having low preference even if the input stimulus has high contrast, i.e. false-positive responses, in order to discriminate among two ambiguous cases described above.

III. INHIBITION OF FALSE-POSITIVE RESPONSES

The model proposed in this paper is composed of three layers and three processing stages that are executed on the

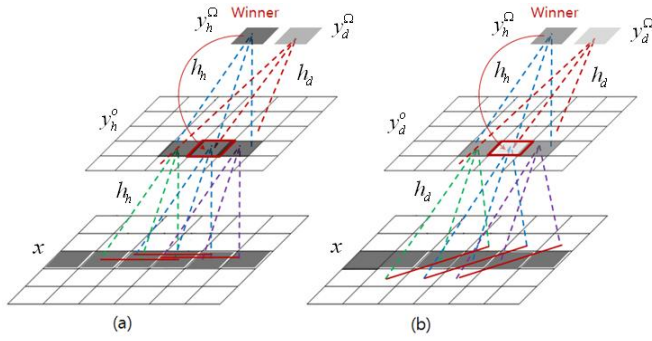


Fig. 4. (a) Horizontal orientation channel at the output layer is reconvolved with filters tuned for horizontal and diagonal edges respectively. (b) Diagonal orientation channel at the output layer is reconvolved with filters tuned for horizontal and diagonal edges respectively.

basis of the connection between those three layers. The three layers are the input, output and Ω -layers. The input and output layers interact through a feed-forward connection, where orientation channels in output layers are connected laterally and output and Ω -layers are linked by feed-forward and feedback connections. In this section, we describe our model in terms of the three processing stages, namely the feed-forward, lateral and feedback stages.

A. Feed-forward Stage

The output layer is composed of a set of orientation channels. The responses of each channel are initialized by classical convolution of the input image and a filter tuned for detecting a particular orientation range of the edge. The number of orientation channels thus depends on the number of filters. The aim of the feed-forward stage is to pass through as many edges with true orientation as possible even though edges with false orientation are passed as well. This is because our model provides a mechanism to suppress false-positive responses in the lateral and feedback stages. As described in section 3.B, while the Gabor filtering sometimes prevents true edges from activating, Neumann filtering passes through as many true edges as possible. Therefore, we employed Neumann filtering for the feed-forward stage. Figure. 3 shows input and output layers, in which (a) and (b) depict the feed-forward stage based on convolution. The N orientation channels at the output layer are initially determined by the feed-forward stage for all $\theta = \{0, \pi/N, \dots, (N-1)\pi/N\}$:

$$y_{\theta}^o = y_{\theta}^{ff}, \quad (5)$$

where ff denotes feed-forward stage and y_{θ}^{ff} is computed by Neumann filtering.

B. Lateral Inhibition Stage

In this subsection, we focus on the role of lateral interaction inhibiting false-positive responses generated from the feed-forward stage. There is a horizontal line in the input image x of Fig. 3. In (a), the response in the horizontal orientation channel y_h^o is large because the input is convolved

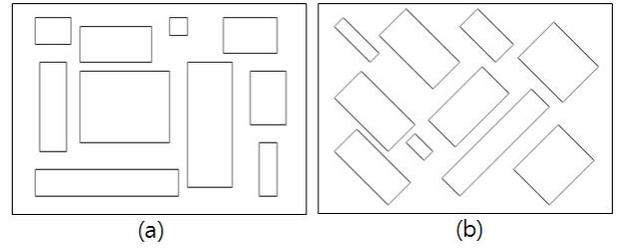


Fig. 5. (a) Artificial image composed only of edges with orientations of 0° and 90° . (b) Artificial image composed only of edges with orientations of 45° and 135° .

with a filter that prefers a horizontal line. On the other hand, the response in the diagonal orientation channel y_d^o is relatively small. If the black rectangle in y_h^o is the winner cell among orientation channels at the spatial position, then this winner inhibits cells with the same position in the rest of orientation channels.

The response of the lateral inhibition stage l at the spatial position (m, n) of the orientation channel θ is defined as

$$y(m, n)_{\theta}^l = y(m, n)_{\theta}^o \quad \text{if } y(m, n)_{\theta}^o / y(m, n)_{max}^o > T^l \\ y(m, n)_{\theta}^l = y(m, n)_{\theta}^o \cdot e^{-(y(m, n)_{max}^o - y(m, n)_{\theta}^o) / k} \quad \text{else} \quad (6)$$

where $y(m, n)_{max}^o$ denotes the maximum value over all orientation channels at spatial positions (m, n) . k is a constant to mediate the inhibition rate. $y(m, n)_{\theta}^o$ is preserved if $y(m, n)_{\theta}^o / y(m, n)_{max}^o$ is larger than the threshold T^l . Otherwise, $y(m, n)_{\theta}^o$ is inhibited. The level of inhibition depends on the difference between the responses of the target cell and the winner. As the difference becomes larger, the output value of the target cell is strongly suppressed. Unlike the *winner-take-all*, this restricts inhibition to cells under a certain threshold, because true responses are often eliminated when *winner-take-all* process is subsequently applied after the feed-forward stage. Each orientation channel at the output layer $y(m, n)_{\theta}^o$ is replaced by $y(m, n)_{\theta}^l$ after the lateral inhibition stage.

C. Inhibitory Feedback Stage

The Ω -layer is composed of a set of orientation channels denoted by y_{θ}^{Ω} . The number of orientation channels is $N * N$, where N is the number of oriented filters. Figure. 4 (a) shows the three layers of our model. In the feedback stage, the horizontal orientation channel y_h^o is reconvolved with the filters preferring the horizontal and the diagonal edge in that order. The response of the red rectangle in y_h^o is not inhibited when the response of y_h^o at the same spatial position is highest among all orientation channels of the Ω -layer. Figure. 4 (b) shows that responses in the diagonal orientation channel. y_d^o are reconvolved with the filters preferring the horizontal and the diagonal edge in that order. The response of the red rectangle in y_h^o is inhibited when the response of y_h^o at the same orientation and position is not highest among all the orientation channels of the Ω -layer. The response of

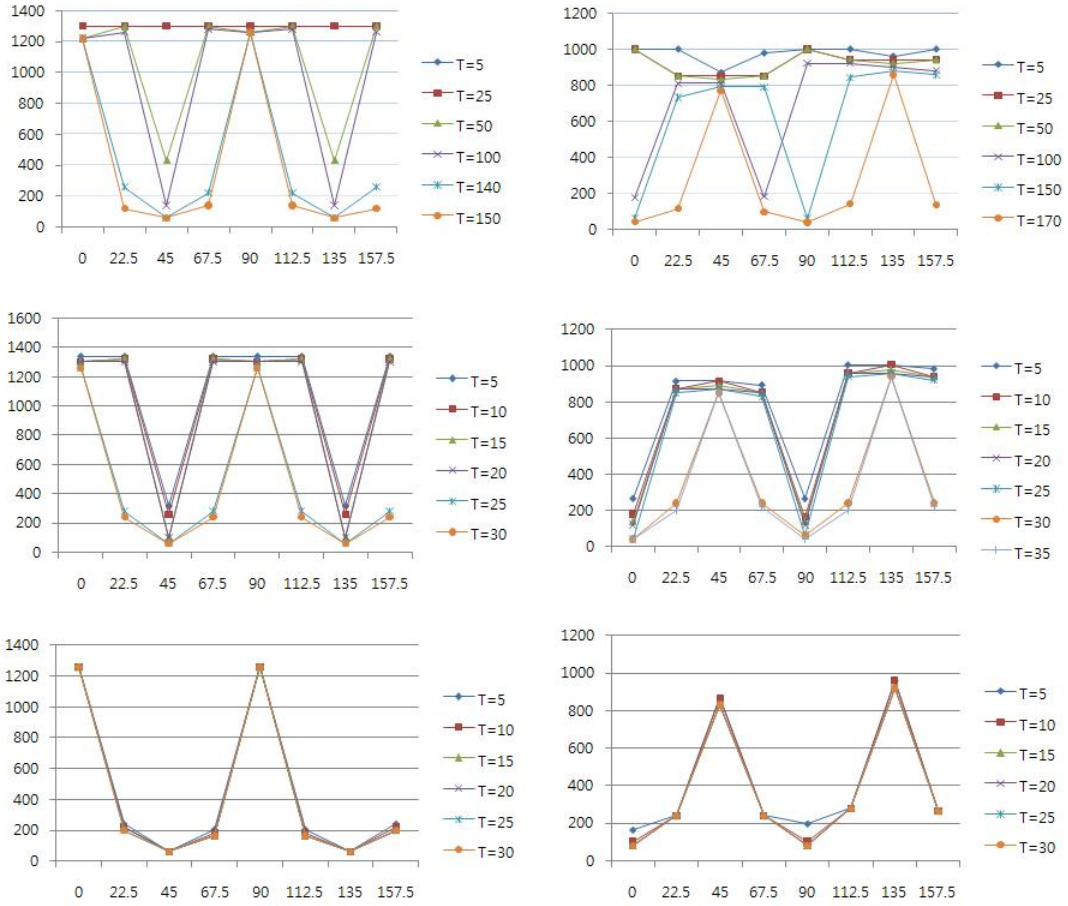


Fig. 6. The Y-axis of each graph represents number of responses which are higher than a particular intensity value. The X-axis is output orientation and T denotes the intensity threshold. The graphs in the first and second columns are obtained using Fig. 5 (a) and (b), respectively. Three rows show results from Neumann, Gabor and proposed filtering, respectively.

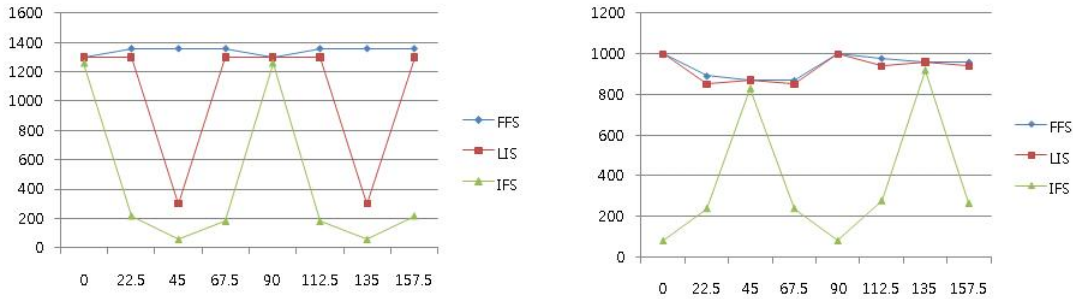


Fig. 7. Graphs obtained by using the proposed filtering scheme with (a) and (b) in Fig. 5, respectively. Both cases have T=10.

the orientation channel θ and the spatial position (m, n) at the feedback stage fb is defined as

$$\begin{aligned}
 y(m, n)_{\theta}^{fb} &= y(m, n)_{\theta}^o \quad \text{if } y(m, n)_{max}^{\Omega} \wedge max = \theta \\
 y(m, n)_{\theta}^{fb} &= 0 \quad \text{else}
 \end{aligned} \quad (7)$$

In feedback stage, a response of the output layer is not suppressed if the response of that orientation and position at the Ω -layer is the largest while a response of the output layer is inhibited if the response of that orientation and position at

the Ω -layer is not the largest. The connections between the output and Ω -layer encode some intuition that is relevant to the shape made by the responses of each orientation channel in the output layer. For example, collinearly aligned responses in the horizontal channel in the output layer must be oriented in the horizontal direction if the responses are correct. Ideally, since the horizontal orientation channel contains edges oriented towards the horizontal direction, the main axis of collinearly aligned responses in the horizontal channel should be horizontal.

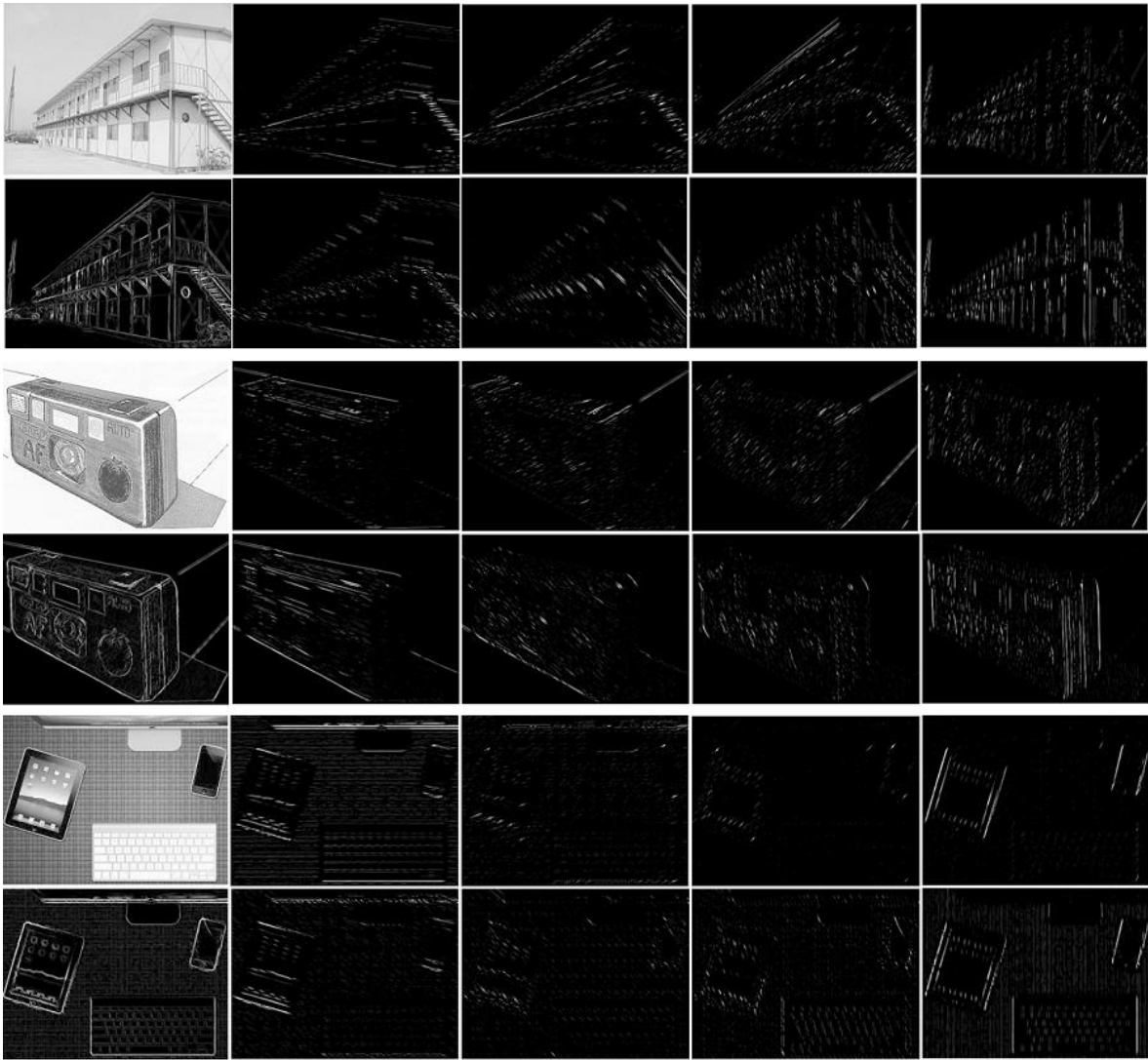


Fig. 8. The left column contains the three original images; building, camera, and desk. The three images below each original image are generated by max pooling over all orientations. The image to right of each original image is the 0 orientation channel and then orientation is increased clockwise e.g. $0^\circ, 22.5^\circ, \dots, 157.5^\circ$.

To summarize, the hypothesis behind the feedback stage is that collinearly aligned responses of a particular orientation channel have to be oriented in the direction of the channel at the output layer if they are not false-positive responses. Therefore, reconvolution is executed on orientation channels in the output layer to detect responses consistent with this hypothesis, otherwise the response is inhibited. For the actual implementation, the oriented Gaussian used in the simple cell step of the feed-forward stage is applied to the reconvolution operation.

IV. EXPERIMENTS

A. Experimental Setup

We compared the performance of our model with that of Gabor and Neumann filtering. All filtering schemes used eight oriented filters ($0^\circ, 22.5^\circ, 45^\circ, \dots, 157.5^\circ$) and the range of responses was from 0 to 255. The parameters $\sigma = 2.0$ and $\lambda = 0.15$ in equation (3) were chosen for both feed-forward

and feedback stages and the parameters $\sigma_x = 1.4$, $\sigma_y = 2.5$, and $u_0 = 0.4$ in equation (1) were selected for Gabor filtering. Furthermore, we measured the performance in each stage. To do this, we refer to the three stages in our model as: (1) FFS (Feed-forward stage), (2) LIS ((1) + lateral inhibition stages) and (3) IFS ((2) + Inhibitory feedback stage). All images used in experiments have a resolution of 320x240.

B. Performance Evaluation with Artificial Images

We evaluated the model performance in the quantitative and qualitative aspect with artificial and natural images. Figure. 5 shows two artificial images; (a) is composed only of edges with an orientation of 0° and 90° , where the number of pixels oriented towards 0° and 90° is 1180 and 1220, respectively, and (b) consists only of edges with an orientation of 45° and 135° , where the number of pixels oriented towards 45° and 135° is 820 and 770, respectively.

Comparative performance results of the three filtering

schemes are shown in Fig. 6, where graphs in the three rows were obtained by Neumann filtering, Gabor filtering, and the proposed filtering method, respectively. The left and right columns show results from using Fig. 6(a) and (b). The Y-axis of each graph represents the number of responses that are higher than a particular intensity threshold. In other words, it represents how many pixels above an intensity threshold value are activated in an orientation channel. Ideally, graphs in first column should have high values for orientations of 0° and 90° while the other orientations should have zero values with a very low intensity threshold. Similarly, graphs in the second column should have high value only for orientations of 45° and 135° with a very low threshold. Neumann filtering shows poor performance compared to this ideal scenario described. Ideal conditions are achieved by increasing the intensity thresholds up to 140 and 170. The performance of Gabor filtering is better than that of Neumann filtering. With thresholds set to 25 and 30, the ideal conditions were obtained. The performance of the proposed filtering method is clearly the best among the three filtering schemes. With thresholds set to 5 and 10, the ideal conditions were achieved. The results show that false-positive responses are successfully suppressed by the proposed model.

From a different perspective, it is important to not only inhibit false-positive activities but also to preserve true responses. As is shown in the true orientation channels of both left and right columns, the number of true responses produced by our model is almost equal to that obtained using other approaches. This suggests that true responses are not suppressed during the two proposed inhibition stages. Figure.7 shows a performance comparison of the three steps involved in our model. It is noted that lateral stage can effectively reduce false-positive responses as can be seen from the left graph. It can also be ineffective as can be seen from right graph. However, most remained false-positives are inhibited through the feedback stage.

C. Performance Evaluation with Natural Images

Next, we evaluated the model performance in the qualitative aspect. As shown in Fig. 8, we applied our model to three natural images, i.e. building, camera and desk. Each orientation channel and image obtained from max pooling over all orientations demonstrate that our model achieves reasonable qualitative performance in terms of passing edges inside the target orientation band and preserving edges that should be detected. The responses in each orientation channel are in good qualitative agreement with human intuition and it seems that edges of true orientation are rarely eliminated during the proposed inhibition stages since the image obtained from max pooling contains most edges from the original image.

V. CONCLUSIONS AND FUTURE WORKS

We proposed a computational model based on the basic mechanisms of cortical processing, i.e. feed-forward, lateral and feedback stages, in order to inhibit false-positive responses returned by the classical filter-based approach. Our

model was evaluated experimentally and was compared with Gabor and Neumann filtering. In the experiments, various artificial and natural images were used and the number of false-positive responses was compared to evaluate the performance of each filtering scheme. The results validated the effectiveness of our approach.

In future work, we plan to include recurrent connections in our model to build it on a more biologically plausible architecture and to achieve better and reliable performance in terms of inhibition of false-positive responses. In addition, we will extend our model for multiple orientation detection and noise tolerance.

VI. ACKNOWLEDGMENTS

This work was supported by the Global Frontier R&D Program on <Human-centered Interaction for Coexistence> funded by the National Research Foundation of Korea grant funded by the Korean Government (MEST) (NRF-M1AXA003-2011-0028353). All correspondences should be addressed to I. H. Suh.

REFERENCES

- [1] D. G. Lowe. Distinctive image features from scale-invariant keypoints. *IJCV*, 60(2):91-110, 2004.
- [2] Navneet Dalal and Bill Triggs. Histograms of Oriented Gradients for Human Detection. In *CVPR*, pages 886-893, 2005.
- [3] D. George. How the brain might work: A hierarchical and temporal model for learning and recognition, Ph.D. dissertation, Stanford Univ., Stanford, CA, 2008.
- [4] Serre, L. Wolf, S. Bileschi, M. Riesenhuber, and T. Poggio. Robust object recognition with cortex-like mechanisms, *IEEE Trans. Pattern Anal. Machine Intell.*, vol. 29, no. 3, pp. 411426, 2007.
- [5] Hansen T, Neumann H. A recurrent model of contour integration in primary visual cortex. *Journal of Vision*. 2008;8:125.
- [6] J. G. Daugman. Uncertainty relation for resolution in space, spatial frequency, and orientation optimized by two-dimensional visual cortical filters. *Journal of the Optical Society of America A*, 2(7):11601169, July 1985.
- [7] H. Knutsson. Representing Local Structure Using Tensors, *Proceedings of Scandinavian Conference on Image Analysis*, Oulu, Finland ; June, 1989.
- [8] Contour Detection and Hierarchical Image Segmentation P. Arbelaez, M. Maire, C. Fowlkes and J. Malik. *IEEE TPAMI*, Vol. 33, No. 5, pp. 898-916, May 2011.
- [9] F. J. Canny. A computational approach to edge detection. *IEEE Trans. Pattern Anal. Machine Intell.*, 8(6):679-698, 1986
- [10] Papari, G., Campisi, P., Petkov, N., and Neri, A. Contour Detection by Multiresolution Surround Inhibition. In *Proceedings of ICIP*. 2006, 749-752
- [11] P. Dollar, Z. Tu, and S. Belongie, Supervised learning of edges and object boundaries, *CVPR*, 2006.
- [12] Gonzalez, R.C., P. Wintz, *Digital Image Processing*. 2nd Ed., Addison-Wesley, Reading:MA, 1987.
- [13] Bosking, W. H., Zhang, Y., Schofield, B., and Fitzpatrick, D. Orientation selectivity and the arrangement of horizontal connections in tree shrew striate cortex. *Journal of Neuroscience*, 17(6):21122127. (1997).
- [14] Pettet, M. W., McKee, S. P., and Grzywacz, N. M. Constraints on long range interactions mediating contour detection. *Vision Research*, 38:865879. (1998).
- [15] Ben-Yishai R, Bar-Or RL, Sompolinsky H.. Theory of orientation tuning in visual cortex. *Proc. Natl. Acad. Sci. USA* 92: 384448. 1995.
- [16] Somers DC, Nelson SB, Sur M.. An emergent model of orientation selectivity in cat visual cortical simple cells. *J. Neurosci.* 15:544865. 1995.
- [17] Wallace, J., Stone, L. and Masson, G. Object motion computation for the initiation of smooth pursuit eye movements in humans. *Journal of Neurophysiology*, 93, 22792293. (2005).